Photodegradation of dyes by a novel TiO_2/*u*-RuO_2/GNS nanocatalyst derived from Ru/GNS after its use as catalyst in aerial oxidation of primary alcohols (GNS = graphene nanosheets)

Mayakrishnan Gopiraman • Sundaram Ganesh Babu • Zeeshan Khatri • Byoung-Suhk Kim • Kai Wei • Ramasamy Karvembu • Ick Soo Kim

ABSTRACT Ruthenium nanoparticles (RuNPs) supported on graphene nanosheets (GNS) composite (Ru/GNS) was prepared by dry synthesis method and was used as a nanocatalyst for the aerial oxidation of various primary alcohols. The Ru/GNS was highly efficient, selective, stable and heterogeneous in nature. Owing to the high stability of the used catalyst (*u*-Ru/GNS), it was further applied in a different catalytic system *viz* photocatalytic degradation, after suitable modifications. We have obtained a novel TiO_2/*u*-RuO_2/GNS catalyst from *u*-Ru/GNS by sol-gel method. The catalytic activity of TiO_2/*u*-RuO_2/GNS toward the photodegradation of methyl orange (MO) and acridine orange (AO) was found to be an excellent. Overall, the sustainable use of these recyclable materials (Ru/GNS and TiO_2/*u*-RuO_2/GNS) could lead to economic and environmental benefits.

Keywords Graphene nanosheets · Ruthenium oxide nanoparticles · Aerial oxidation · Recycling · Titania · Photocatalytic degradation

M. Gopiraman • S. Ganesh Babu • Z. Khatri • I. S. Kim

Nano Fusion Technology Research Lab, Division of Frontier Fibers, Institute for Fiber Engineering (IFES), Interdisciplinary Cluster for Cutting Edge Research (ICCER), National University Corporation Shinshu University, Ueda, Nagano 386 8567, Japan

e-mail: kim@shinshu-u.ac.jp

S. Ganesh Babu

SRM Research Institute, SRM University, Kattankulathur 603203, India

B. S. Kim

Department of Organic Materials & Fiber Engineering, Chonbuk National University, 561-756 Jeollabuk-do, Republic of Korea

K. Wei

College of Textile Clothing Engineering, Soochow University, Suzhou, 215021, China

R. Karvembu

Department of Chemistry, National Institute of Technology, Tiruchirappalli 620 015, India

e-mail: kar@nitt.edu

Introduction

Till date, several carbon materials (CMs) supported metal nanoparticles (MNPs) based nanocomposites (MNPs/CMs) have been developed to catalyze a wide range of organic transformations [1–3]. Notably, due to specific higher surface area and conductive nature, these MNPs/CMs have played a most promising role as nanocatalysts in photocatalysis [4–6]. Particularly, among the CMs, due to the amazing physicochemical properties, graphene has been receiving greater attention [7–13]. In fact, the MNPs/CMs are highly efficient, reusable, stable and selective heterogeneous catalysts in various organic transformations [14, 15]. But the cost of these hybrid materials is quite high. However, since the materials are stable and active even after the catalytic reactions, they can be tuned to obtain a new active material for further applications. Indeed, from an economical and environmental point of view, sustainable use of already existing materials is very important. Several recycling techniques have been developed and discussed in many review articles [16–18]. Very recently, Princaud and co-workers have highlighted the importance of the recycling of carbon materials and their composites [19]. We have prepared various MNPs/CMs composites which were used as nanocatalysts for various organic transformations [20, 21, 8–10]. Among them, RuNPs supported on GNS composite (Ru/GNS) showed a superior catalytic activity towards aerial oxidation of alcohols, mainly, secondary alcohols [8]. Moreover, we found that the Ru/GNS is highly reusable, stable and easily tunable. Hence, in this study, we have carried out more investigation on the Ru/GNS catalyst. At first, the Ru/GNS was used as a nanocatalyst for the aerial oxidation of primary alcohols. After this catalytic reaction, the used catalyst (*u*-Ru/GNS) was redecorated with TiO_2 for photocatalytic application. In fact, TiO_2 has a relatively high energy band gap and it needs high energy to get excited [22]. RuO_2 may act as a co-catalyst and assist for the better photocatlytic activity of the

TiO_2 [22]. The MO and AO are very stable organic dyes which are extensively used in the pigmentation of textile, leather, paper, cosmetic, ink, ceramic and food-processing products, and high resistant to biodegradation [23–25]. To reduce the environmental problems caused by these dyes, the degradation of such dye molecules into some simple non-toxic molecules is very important. We therefore propose a method to fix this problem by a simple photocatalytic degradation using a novel material (TiO_2/*u*-RuO_2/GNS) prepared from *u*-Ru/GNS.

Experimental

Materials and characterization

Graphene nanoplatelets (GNPs, purity: >99wt%, average thickness: 3 nm, layers: <5, diameter: 1-2 um) were purchased from Cheap tubes Inc., VT, US. H_2SO_4 (98%) and HNO_3 (70%) were purchased from Wako pure chemicals, Japan. $Ru(acac)_3$ (97%) and all other chemicals were purchased from Aldrich and used as received.

The surface morphology of the prepared nanocatalysts was investigated by transmission electron microscopy (TEM, JEM-2100 JEOL Japan) with accelerating voltage of 200 kV. The weight percentage of metal NPs on GNS was confirmed by scanning electron microscopy-energy dispersive spectrum [SEM-EDS, Hitachi (model-3000H)]. The chemical state of metal NPs in nanocatalysts was investigated by using X-ray photoelectron spectrum (Kratos Axis-Ultra DLD model instrument). Prior to the XPS analysis, the samples were irradiated under Mg Kα ray source. In order to determine the conversion of the reactants, Gas chromatograms (GC) were recorded using Shimadzu-2010 gas chromatograph. The GC was equipped with 5% diphenyl and 95% dimethyl siloxane, Restek-5 capillary column (0.32 mm dia, 60 m in length) and a flame ionization detector (FID), and nitrogen gas was used as a carrier gas. The initial column

temperature was increased from 60 to 150°C at the rate of 10°C/min and then to 220°C at the rate of 40°C/min. During the product analysis, the temperatures of the FID and injection port were kept constant at 150 and 250°C, respectively. The specific surface area (BET method), specific pore volume and average pore diameter (BJH method) of the sample were measured by N_2 adsorption-desorption isotherms using Quantochrome Autosorb 1 sorption analyzer. Before the measurements, the samples were outguessed at 250°C under vacuum (10-5 mbar) for 3 h. For the photo degradation study, Hitachi U-3500 UV-visible spectrophotometer was used.

Preparation of Ru/GNS

The preparation of Ru/GNS was previously reported by us [8]. In a general procedure, initially, the bi and few layered GNS were obtained from GNPs by a solution phase exfoliation method using *N*–methylpyrrolidone as a solvent. Then the resultant GNS (0.5 g) were chemically treated with a 3:1 volume ratio mixture of concentrated H_2SO_4 and HNO_3. The mixture was sonicated at 40^0C for 3 h in an ultrasonic bath. After cooling to room temperature, the reaction mixture was diluted with deionized water and then vacuum-filtered to obtain the functionalized GNS (*f*-GNS). After that, 0.13 g of $Ru(acac)_3$ was added into 0.5 g of *f*-GNS and mixed well by a mortar and pestle under ambient condition. The homogeneous mixture of *f*-GNS and $Ru(acac)_3$ was obtained within 10-15 minutes. The impregnated $Ru(acac)_3$ was thermally decomposed into metallic RuNPs by calcination at 300°C for 3 h under argon atmosphere.

Aerial oxidation of primary alcohols

A 5.0 mg of Ru/GNS (0.036 mol% of Ru), substrate (1.0 mmol) and toulene (3 mL) were refluxed at 110°C. The completion of the reaction was monitored by TLC. Once the reactions are

completed, the Ru/GNS was separated out from the reaction mixture by simple centrifugation and the products and unconverted reactants were analyzed by GC without any purification. Selectivity of the product for each reaction was also calculated. Finally, the separated nanocatalyst (*u*-Ru/GNS) was washed well with diethyl ether, dried at 130°C for 3 h and was used for the preparation of TiO_2/*u*-RuO_2/GNS.

Preparation of TiO_2/*u*-RuO_2/GNS

The preparation of TiO_2/*u*-RuO_2/GNS nanocatalyst was carried out using a sol-gel method [26]. In a typical procedure, 100 mg of *u*-Ru/GNS was mixed with 14 mL of isopropanol. Simultaneously, another solution was prepared by dissolving titanium tetraisopropoxide (TTIP) (100 mg) in 14 mL of isopropanol. Both the solutions were mixed immediately and added 10% HCl (0.75 g), then stirred vigorously at room temperature for 2 h to obtain a homogeneous solution. Further water was added for the complete hydrolysis of TTIP. The resultant precipitate (TiO_2/*u*-RuO_2/GNS) was filtered and dried at 110°C overnight followed by calcination under N_2 atmosphere at 450°C for 6 h.

Photocatalytic activity of TiO_2/*u*-RuO_2/GNS

In a typical procedure, 25 mg of TiO_2/*u*-RuO_2/GNS was added to 50 mL of 10 mg/L dye solution (MO or AO). Then the solution mixture was magnetically stirred in the dark for 10 min to reach adsorption equilibrium. Subsequently, the stirring was continued under UV (365 nm) light at room temperature. At the given time intervals, 1.5 mL of dye solution was taken out and centrifuged at 6000 rpm for 5 min to remove the residual TiO_2/*u*-RuO_2/GNS. The centrifuged samples were immediately analyzed using UV–visible spectrophotometer.

Results and discussion

Characterization of Ru/GNS

The TEM images (Fig. 1) of Ru/GNS show that the ultra-fine RuNPs were homogeneously attached on the surface of the GNS. The size of RuNPs was found to be 0.5-3.0 nm with a mean diameter of 1.9 nm. The I_D/I_G ratio of Ru/GNS was about four times higher than

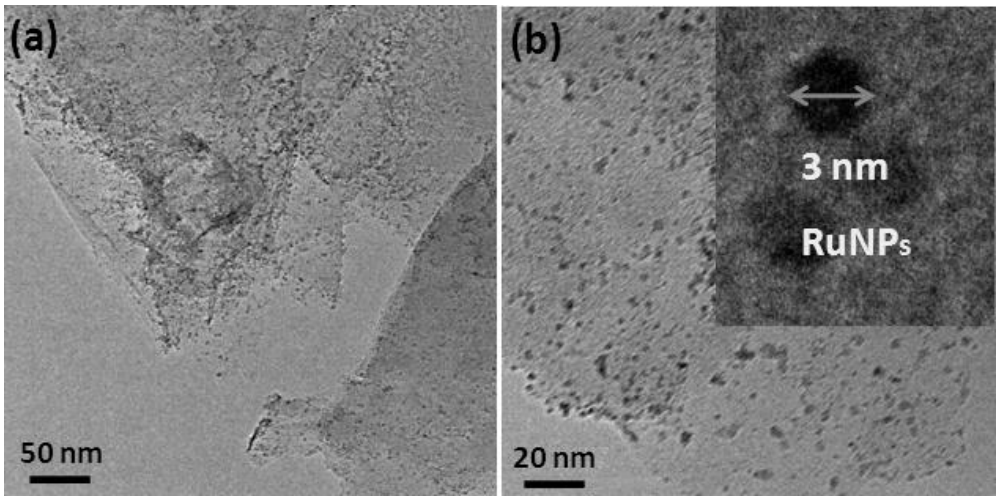

Fig. 1 TEM images of Ru/GNS

that of acid treated GNS (*f*-GNS), and in comparison to the *f*-GNS, a positive shift in G band (from 1570 to 1578 cm^{-1}) was observed in the Raman spectrum of Ru/GNS(Fig. S1), which confirmed the attachment of RuNPs on the surface of GNS. From the SEM-EDS analysis (Fig. S2), the weight percentage of Ru in Ru/GNS was found to be 3.31 wt%. The XPS spectrum of Ru/GNS (Fig. S3) showed BE for Ru $3p_{3/2}$ at 461.0 eV and Ru $3p_{1/2}$ at 483.2 eV, which correspond to the photoemission from metallic Ru. The Ru/GNS has a BET surface area of 83.3 m^2g^{-1} with a pore volume of 0.392 cm^3g^{-1} and a BJH desorption average pore diameter of 19 nm which correspond to literature values [8].

Ru/GNS catalyzed aerial oxidation of alcohols

The optimized reaction conditions were adopted from our previously reported procedure [8]. Fortunately, under the optimized reaction conditions [alcohol (1 mmol), Ru/GNS (0.036 mol%), toluene (3 mL), 110°C], benzyl alcohol gave the corresponding benzaldehyde in an excellent yield of 95% (Table 1, entry 1) without any over oxidation. On the other hand, the cobalt-doped birnessite (Co-Bir) catalytic system gave 84% of the same product from benzyl alcohol only after 24 h even under aerobic condition [27]. Similarly, benzyl alcohols containing substituents such as $–NO_2$, $–OCH_3$ or $–CH_3$ at *para* position were effectively oxidized to the corresponding aldehydes in good to moderate yields without affecting the selectivity (Table 1, entries 2–4). Nevertheless lesser selectivity (79%) was experienced with nickel oxide doped hydroxyapatite (NiO-HAP) catalyst towards the oxidation of 4-nitrobenzyl alcohol [28]. It was found that pyridin-4-ylmethanol was oxidized to its corresponding aldehyde in good yield of 79% (Table 1, entry 5). It is worth mentioning that less reactive aliphatic alcohols were transformed to the corresponding aldehydes in moderate to good yields, but the selectivity was excellent (Table 1, entries 6-10). But RuO_2/V_2O_5 nanocatalyst took 31 h for the aerial oxidation of an aliphatic alcohol (2-octanol) to get 83% conversion [29]. Similarly, aliphatic alcohol oxidation was very meager in Ru(III)/NMO catalytic system [30]. Likewise AuNPs supported Mg-Al-layered double hydroxide (Au/LDH) aerobic oxidation system was inactive towards the conversion of 1-hexanol to 1-hexanone [31]. In the transformation of cyclopropylmethanol to cyclopropanecarbaldehyde (Table 1, entry 11), the present Ru/GNS system gave a good yield of 88% with 100% selectivity. Interestingly, 65% of 2-(furan-2-yl)acetaldehyde was obtained from the oxidation of 2-(furan-2-yl)ethanol (Table 1, entry 12). These results showed the effectiveness of the Ru/GNS catalyst towards the oxidation of primary alcohols.

Table 1. Oxidation of alcohols[a]

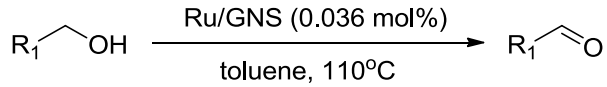

entry	substrate	product	time (h)	conv.[b] (%)	sel.[b] (%)	yield[b] (%)
1	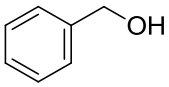	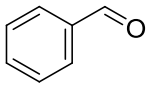	18	95	100	95 (89)[c]
2	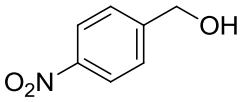	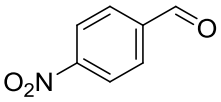	18	82	100	82 (77)
3	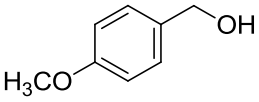	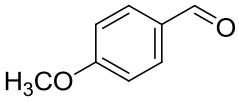	20	81	100	81 (79)
4	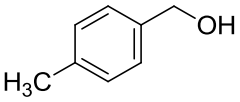	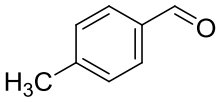	24	75	87	62 (54)
5	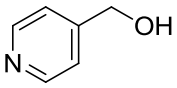	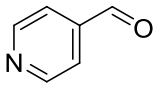	24	79	100	79 (76)
6	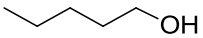	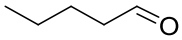	18	83	94	77
7	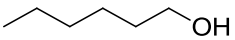	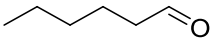	22	85	100	85
8	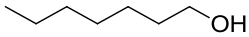	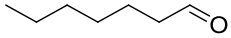	22	82	100	82
9	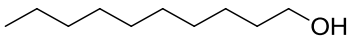	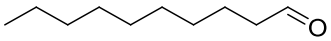	24	71	89	60
10	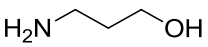	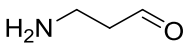	24	97	100	97 (93)
11	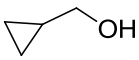	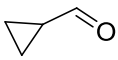	18	88	100	88
12	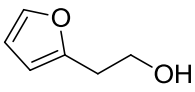	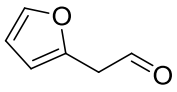	20	77	88	65

[a] Reaction conditions: Substrate (1 mmol), Ru/GNS (0.036 mol%), toluene (3 mL), 110°C.

[b] Determined by GC analysis. [c] Isolated yield is given in paranthesis.

Characterization of TiO_2/*u*-RuO_2/GNS

The TEM images [Fig. 2(a-c)] of TiO_2/*u*-RuO_2/GNS showed a small and homogeneously dispersed RuO_2NPs and TiO_2NPs on GNS. The size of the RuO_2NPs and TiO_2NPs was found in the range of 3-6 nm and 15-20 nm respectively. The SEM–EDS images and their corresponding elemental mapping were recorded for TiO_2/*u*-RuO_2/GNS [Fig. 3(a) and (b)]. The weight percentage of Ru and Ti was found to be 2.19 and 12.19 respectively. The elemental mapping confirmed that the TiO_2NPs and RuO_2NPs were distributed uniformly on the surface of GNS. The XPS [Fig. 4(a-c)] and XRD [Fig. 5(a)] measurements were carried out to investigate the chemical state of Ti. The BE of Ti $3p_{1/2}$ at 464.5 eV and Ti $3p_{3/2}$ at 458.9 eV were ascribed due to the photoemission from TiO_2 [32]. Moreover, two low intensity peaks centered at 465.8 and 460.2 eV were attributed to Ti-C bond formation. The BE of Ru $3d_{5/2}$ at 208.8 eV, Ru $3p_{3/2}$ at 462.5 eV and Ru $3p_{1/2}$ at 485.0 eV were attributed to the photoemission from RuO_2 (Ru^{4+}). The X–ray diffraction peaks observed at 25.2, 37.9, 47.8, 54.5 and 62.9° correspond to the typical crystal faces (101), (004), (200), (105) and (211) of TiO_2. These diffraction peaks matched well with the crystal structure of the anatase TiO_2 [33, 34]. The calculated Raman intensity ratio (*I*D/*I*G=0.1667) was higher in comparison to *f*-GNS (*I*D/*I*G=0.0909) [Fig. 5(b)], which evidently revealed that the RuO_2NPs and TiO_2NPs interacted with GNS [8]. Besides, new peaks were observed at 300-500 cm^{-1} for TiO_2/*u*-RuO_2/GNS, which attributed to TiO_2.

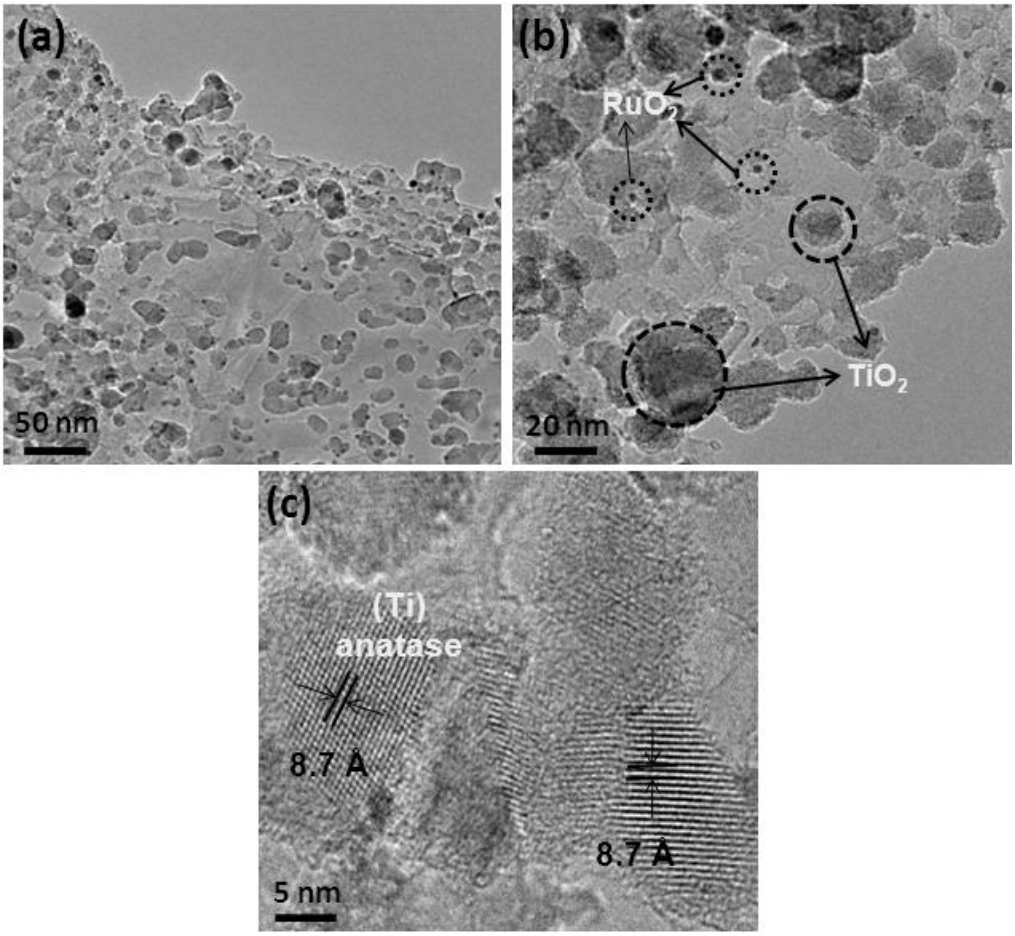

Fig. 2 TEM images of TiO_2/*u*-RuO_2/GNS

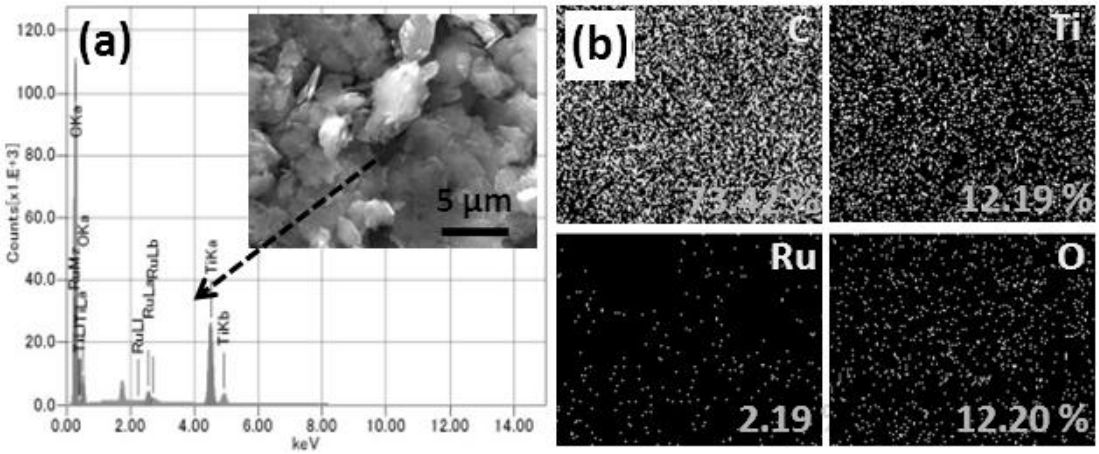

Fig. 3 (a) SEM (inset) and EDS spectrum of TiO_2/*u*-RuO_2/GNS and (b) corresponding elemental mapping observations of C, Ti, Ru and O

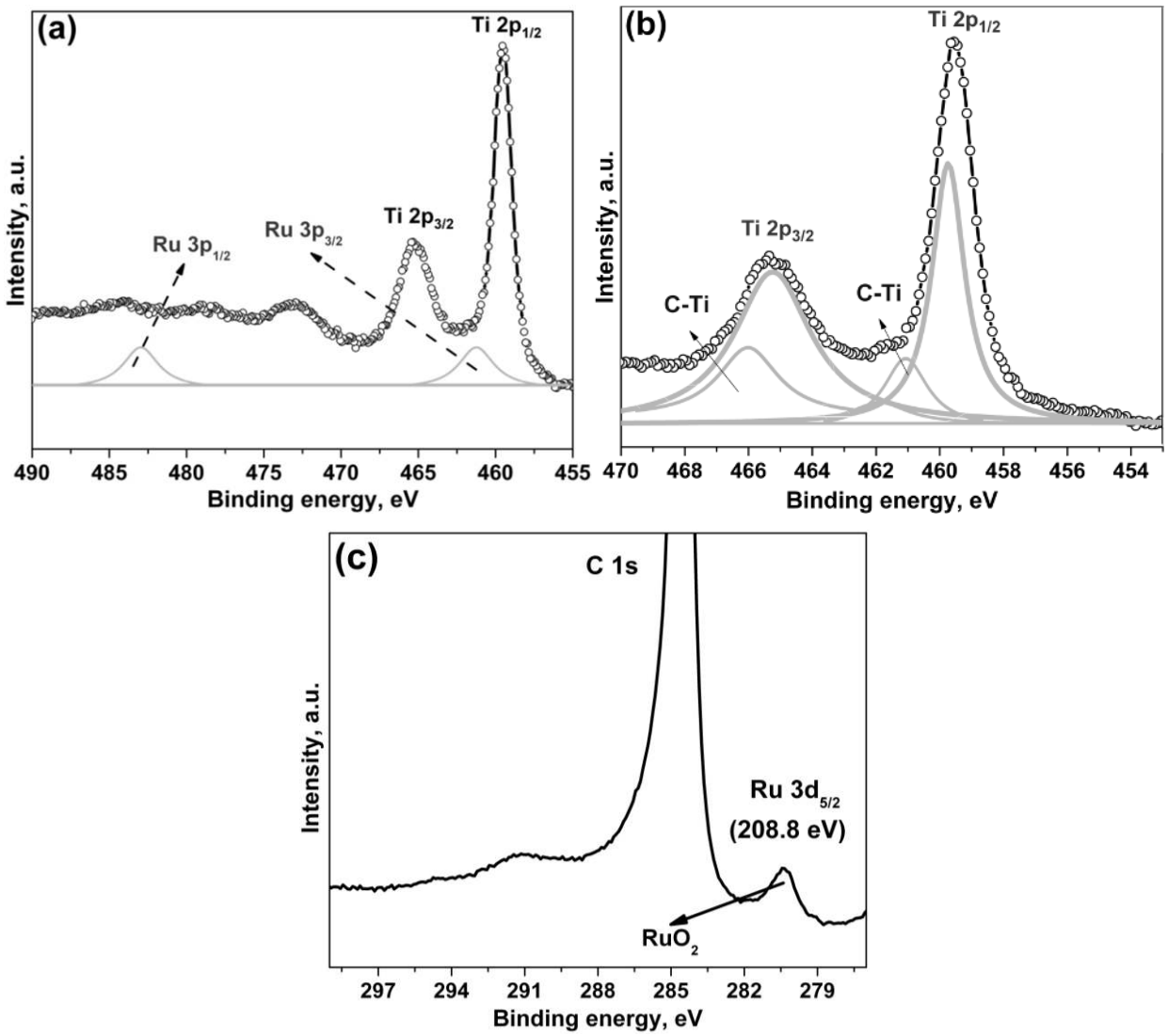

Fig. 4 XPS spectrum of TiO_2/*u*-RuO_2/GNS; main peaks of (a) Ru 3p and Ti 2p, (b) Ti 2p, and (c) C 1s

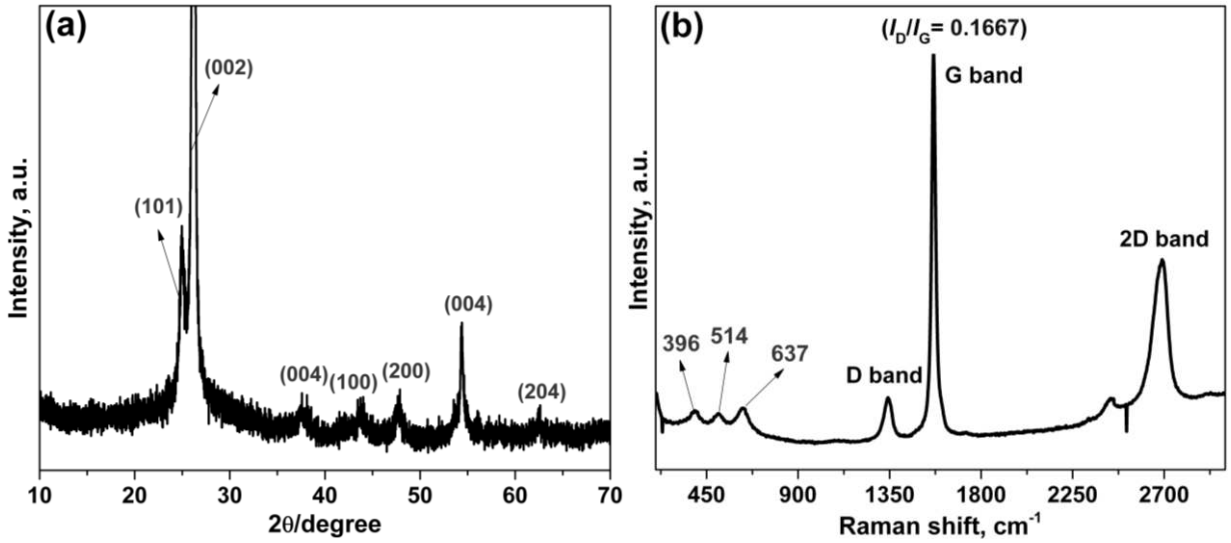

Fig. 5 (a) XRD pattern and (b) Raman spectrum of TiO_2/*u*-RuO_2/GNS

TiO_2/*u*-RuO_2/GNS-catalyzed photodegradation of MO and AO

The UV-visible spectra of TiO_2/*u*-RuO_2/GNS revealed its semiconducting nature with a band gap of 2.92 eV; this moderate band gap is capable enough to consider this as a photocatalyst. The changes in the absorption spectra of the two dyes (MO and AO) during the photocatalytic process at different UV irradiation times are shown in Fig. 6. After TiO_2/*u*-RuO_2/GNS was dispersed in the MO or AO aqueous solutions, the degradation of MO and AO was examined at the characteristic absorption bands, 464 and 492 nm respectively. Initially, the aqueous solutions were stirred under dark condition in order to obtain adsorption/desorption equilibrium and no significant change in the UV-visible spectra of MO and AO was observed (Fig. 6). Whilst under UV irradiation, the intensity of the absorption bands of MO and AO gradually decreased as a function of increasing time, suggesting effective degradation of dye molecules in the presence of UV light. In the present case, TiO_2/u-RuO_2/GNS completely degraded MO into colourless small molecules after UV irradiation for 120 min which is a significant improvement when compared to TiO_2-graphene which has been reported to completely degrade MO after 225 min [35]. A

similar trend was observed with $RuO_2/TiO_2/SiO_2$ photocatalyst, but adequate degradation was reported after 120 min even for 5 mg/L MO solution [36]. Likewise, in the photocatalytic degradation of AO, the present photocatalytic system showed better activity (complete degradation of AO after 12 h) when compared to TiO_2NPs-catalyzed system (complete degradation of AO after 24 h) [37]. Polymeric metalloporphyrins were also utilized as a photocatalyst for the degradation of AO, however the system worked well only in the presence of H_2O_2 (0.4 g/L) under UV light [38]. Otherwise the pH of the solution should be adjusted to 3.0 for the effective decolorization of AO in aqueous solution by Fenton's like reagent (Fe^{2+} and H_2O_2) [39]. As can be seen from Fig. S4 in the supporting information, we were even able to see such degradation by our naked eyes at different time intervals. The TiO_2/*u*-RuO_2/GNS can readily be recovered from the reaction mixture *via* simple filtration and showed good catalytic efficiency even after recycling for three times. There may be three possible reasons for the fast degradation of organic dyes by TiO_2/*u*-RuO_2/GNS: (1) GNS with high charge mobility can act as excellent e− acceptor, is expected to enhance the interfacial e− transfer of RuO_2/TiO_2, (2) the presence of co-catalyst RuO_2, and (3) GNS with very high specific surface area can also enhance the dispersion of catalysts (RuO_2/TiO_2) and permit greater photon absorption on the catalyst surface, leading to the formation of more hydroxyl radicals (•OH) consequently increasing the activity.

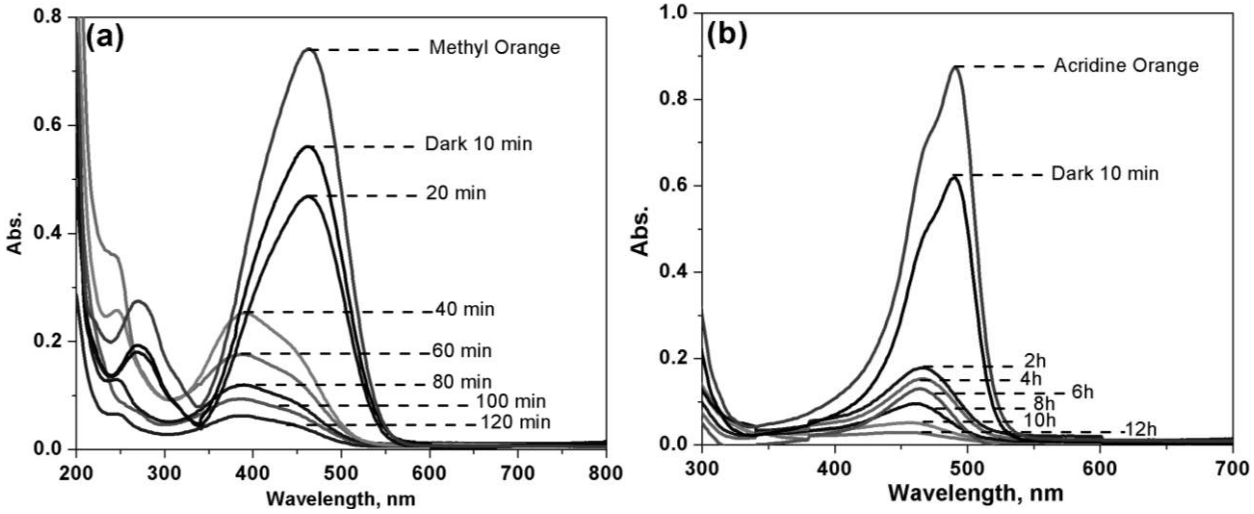

Fig. 6 UV-visible spectrometric evidence for the photodegradation of (a) MO and (b) AO using TiO_2/*u*-RuO_2/GNS under UV light at different time intervals

Plausible mechanism

A tentative mechanism is proposed for TiO_2/*u*-RuO_2/GNS-catalyzed photodegradation of MO and AO, as shown in Fig. 7 and equations 1-5. Initially the photon of energy greater than or equal to the band gap of TiO_2 ($E_{hv} \geq Eg$) was absorbed from the external UV light by the electrons in the valance band of TiO_2 [TiO_2 (e^-_{vb})]. These energized electrons moved to the conduction band of TiO_2 [TiO_2 (e^-_{cb})] and as a result holes were generated in the valance band [TiO_2 (h^+_{vb})]. Subsequently, these photoexcited electrons moved through the GNS layer and utilized for the conversion of oxygen molecule (O_2) to superoxide anion (O_2^-). The high carrier mobility of GNS played a vital role in transporting these electrons and thereby retarded the electron-hole pair recombination. At the same time, the hole in the valance band of TiO_2 [TiO_2 (h^+_{vb})] was combined with an electron from RuO_2. As a result a hole was generated in the co-catalyst, RuO_2, and thus preventing the electron-hole pair recombination further in TiO_2. Then,

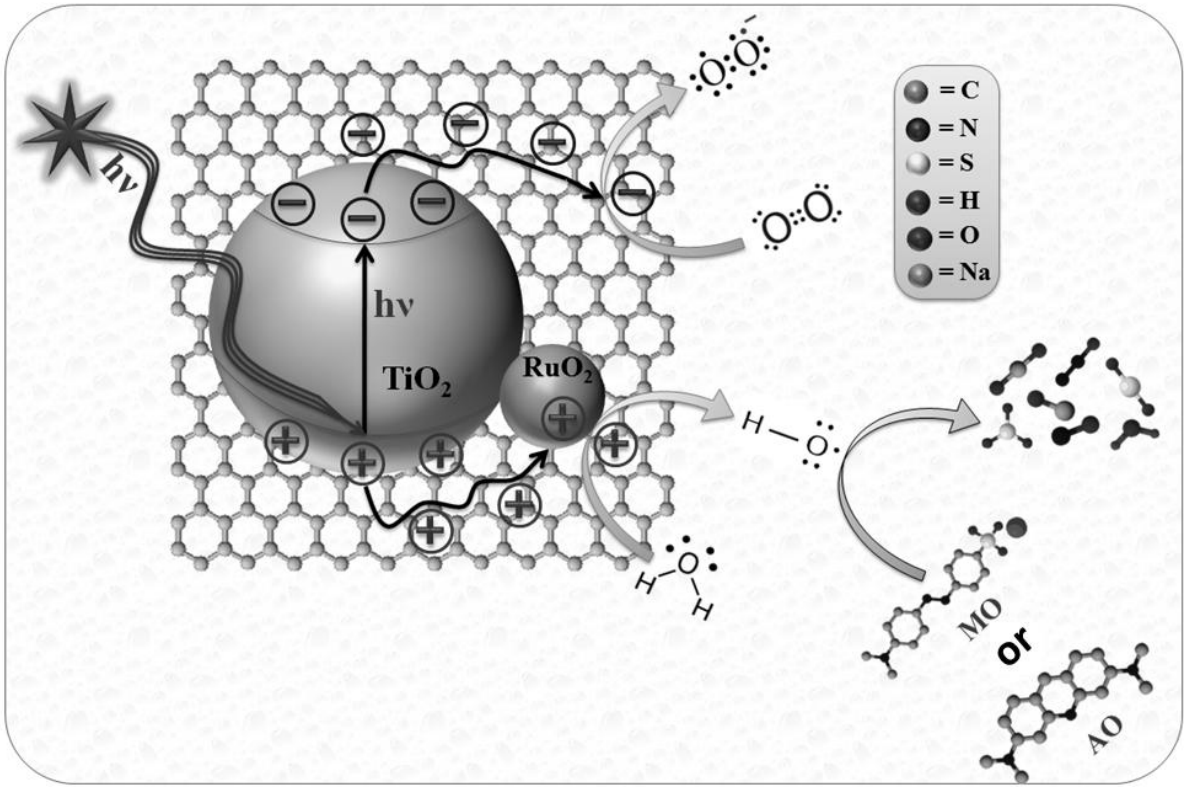

Fig. 7 Photocatalytic degradation of organic pollutants using TiO_2/*u*-RuO_2/GNS

these generated holes in RuO_2 produced hydroxyl radicals (•OH) by reacting with water. The formed •OH radicals are strong oxidants which induced faster oxidation of MO or AO and degradation of the intermediates.

$$TiO_2 + h\nu\ (E \geq Eg) \rightarrow TiO_2\ (e^-_{cb} + h^+_{vb}) \quad (1)$$

$$TiO_2\ (e^-_{cb}) + O_2 \rightarrow O_2^- \quad (2)$$

$$TiO_2\ (h^+_{vb}) \text{ »»»» } RuO_2\ (h^+) \quad (3)$$

$$RuO_2\ (h^+) + H_2O \rightarrow RuO_2 + HO\bullet + H^+ \quad (4)$$

$$HO\bullet + \text{Dye} \rightarrow \text{Degradation products} \quad (5)$$

Conclusions

In summary, the Ru/GNS catalyst showed an excellent activity towards the aerial oxidation of primary alcohols. Interestingly, a novel TiO_2/*u*-RuO_2/GNS catalyst was successfully prepared from the *u*-Ru/GNS and TTIP. The merit of the TiO_2/*u*-RuO_2/GNS catalyst was realized from its excellent photodegradation activity toward MO and AO. The TiO_2/*u*-RuO_2/GNS catalyst is reusable and heterogeneous in nature. The sustainable use of the Ru/GNS and an excellent photocatalytic activity of the TiO_2/*u*-RuO_2/GNS, make these materials economically and environmentally feasible. Moreover, since Ru/GNS and TiO_2/*u*-RuO_2/GNS are highly versatile, they can be applied in various fields.

Acknowledgements

This work was supported by the Grant-in-Aid for Global COE program by the Ministry of Education, Culture, Sports, Science, and Technology, Japan.

Supporting information

Raman, SEM-EDS and XPS spectra are available.

References

1. Serp P, Figueiredo JL (Eds.). (2009) Carbon materials for catalysis, John Wiley & Sons.
2. Rodriguez-Reinoso F (1998) Carbon 36:159−175
3. Jiang Y, Lu Y, Lv X, Han D, Zhang Q, Niu L, Chen W (2013) ACS Catal 3:1263−1271
4. Sakthivel S, Kisch H (2003) Angew Chem Int Ed 42:4908−4911
5. Faria JL, Wang W (2009) Carbon materials in photocatalysis, Carbon materials for catalysis, John Wiley & Sons 481−506
6. Mondal A, Jana NR (2014) ACS Catal 4:593−599
7. Xiang Q, Yu J, Jaronie M (2012) Chem Soc Rev 41:782−796
8. Gopiraman M, Ganesh Babu S, Khatri Z, Wei K, Kim YA, Endo M, Karvembu R, Kim IS (2013) J Phys Chem C 117:23582–23596
9. Gopiraman M, Ganesh Babu S, Khatri Z, Wei K, Morinobu E, Karvembu R, Kim IS (2013) Catal Sci Technol 3:1485–1489
10. Gopiraman M, Bang H, Ganesh Babu S, Wei K, Karvembu R, Kim IS (2014) Catal Sci Technol 4:2099−2106
11. Perera SD, Mariano RG, Vu K, Nour N, Seitz O, Chabal Y, Balkus KJ (2012) ACS Catal 2:949−956.
12. Stengl V, Popelkov D, Vlacil P (2011) J Phys Chem C 115:25209–25218
13. Fotiou T, Triantis TM, Kaloudis T, Pastrana-Martínez LM, Likodimos V, Falaras P, Silva AMT, Hiskia A (2013) Ind Eng Chem Res 52:13991–14000
14. He D, Kou Z, Xiong Y, Cheng K, Chen X, Pan M, Mu S (2014) Carbon 66:312–319
15. Xiong Z, Zhang LL, Ma J, Zhao XS (2010) Chem Commun 46:6099−6101
16. Goto M (2009) J Supercrit Fluids 47:500−507
17. Adschiri T, Lee KW, Goto M, Takami S (2011) Green Chem 13:1380−1390
18. Pimenta S, Pinho ST (2011) Waste Manag 31:378−392

19. Princaud M, Aymonier C, Loppinet-Serani A, Perry N, Sonnemann G (2014) ACS Sustainable Chem Eng 2:1498–1502
20. Gopiraman M, Karvembu R, Kim IS (2014) ACS Catal 4:2118−2129
21. Gopiraman M, Ganesh Babu S, Khatri Z, Kai W, Kim YA, Endo M, Karvembu R, Kim IS (2013) Carbon 62:135–148
22. Yasunobu I, Takao N, Yoshihiro A, Kazunori S (1992) J Chem Soc Chem Commun 7:579−580
23. Xie Y, Chen F, He J, Zhao J, Wang H (2000) J Photochem Photobiol A 136:235–240
24. Faisal M, Tariq MA, Muneer M (2007) Dyes Pigments 72:233–239
25. Li G, Ciston V, Saponjic ZV, Chen L, Dimitrijevic NM, Rajh T, Gray KA (2008) J Catal 25:105–110
26. Jiaguo Y, Xiujian Z, Qingnan Z (2001) Mater Chem Phys 69:25–29
27. Kamimura A, Nozaki Y, Nishiyama M, Nakayama M (2013) RSC Adv 3:468–472
28. Emayavaramban P, Ganesh Babu S, Karvembu R, Dharmaraj N (2014) Adv Sci Eng Med 6:659–666
29. Ganesh Babu S, Krishnamoorthi S, Thiruneelakandan R, Karvembu R (2014) Catal Lett 144:1245–12520
30. Mancuso AJ, Huang SL, Swern DJ (1987) J Org Chem 43:2480–2482
31. Liang W, Xiangju M, Fengshou X (2010) Chin J Catal 31:943–947
32. Ruan S, Wu F, Zhang T, Gao W, Xu B, Zhao M (2001) Mater Chem Phys 69:7–9
33. Nagaveni K, Hegde MS, Ravishankar N, Subbanna GN, Madras G (2004) Langmuir 20:2900–2907
34. Luo LJ, Zhang XJ, Ma FJ, Zhang AL, Bian LC, Pan XJ, Jiang FZ (2015) Reac Kinet Mech Cat 114:311–322
35. Peining Z, Nair SA, Shengjie P, Shengyuan Y, Ramakrishna S (2012) ACS Appl Mater Interfaces 4:581−585
36. Ibhadon AO, Greenway GM, Yue Y (2008) Catal Comm 9:153–157

37. Lu CS, Mai FD, Wu CW, Wu RJ, Chen CC (2008) Dyes Pigments 76:706–713

38. Chen H, Jin X, Zhu K, Yang R (2002) Water Res 36:4106–4112

39. Chen CC, Wu RJ, Tzeng YY, Lu CS (2009) J Chin Chem Soc 56:1147–1155